Journal of Metals, Materials and Minerals, Vol.29 No.2 pp.58-63, 2019

Optical and luminescence investigation of Er^{3+} doped in Na_2O-Al_2O_3-P_2O_5 glasses for photonics material application

Natthakridta CHANTHIMA[1,2], Nuchjaree KIWSAKUNKRAN[1,2], Jakrapong KAEWKHAO[1,2], and Narong SANGWARANATEE[3,*]

[1]*Physics Program, Faculty of Science and Technology, Nakhon Pathom Rajabhat University, Meuang, Nakhon Pathom 73000, Thailand*
[2]*Center of Excellence in Glass Technology and Materials Science, Nakhon Pathom Rajabhat University, Meuang, Nakhon Pathom 73000, Thailand*
[3]*Applied Physics Research Group, Faculty of Science and Technology, Suan Sunandha Rajabhat University, Bangkok 10300, Thailand*

[*]**Corresponding author e-mail:** narong.sa@ssru.ac.th, Phone: +66 (0) 62-614-9951

Received date:
23 May 2018
Revised date:
9 August 2018
Accepted date:
7 January 2019

Keywords:
Erbium
Phosphate glass
Luminescence
McCumber theory

Abstract

Optical and photoluminescence properties of Er^{3+} doped Na_2O-Al_2O_3-P_2O_5 (NAPEr) glasses were prepared by conventional melt quenching technique at 1200°C. The absorption spectra have 11 peaks corresponded to $^4I_{15/2}$ ground state to various excited energy levels. The absorption band at 1537 nm shows highest intensity in near-infrared (NIR) region. Also, it can be observed that the intensity of absorption bands increased on increase in concentrations of Er_2O_3. The Judd-Ofelt (JO) parameters ($\Omega\lambda$, λ = 2, 4, and 6) are calculated using the absorption bands of the Er_2O_3 doped glass compositions. McCumber theory has been applied to determine the emission cross-sections (σe) of the $^4I_{13/2} \rightarrow {}^4I_{15/2}$ transition using the absorption cross-sections (σa). The results of these properties revealed that the glasses doped with Er^{3+} ions are promising candidates for photonics material application.

1. Introduction

Recently, glasses doped with various rare earth (RE) ions as very important photonic materials due to several merits than crystalline competitors due it can be doped with substance higher concentration of rear-earth oxide than in crystal, which does not destroy the structure, low cost production, easy fabrication and forming into desired shape [1]. Among various glass materials such as borate, silicate, phosphate and tellurite. Phosphate glass is an interesting host material due to its high transparency, low dispersion, low viscosity, low melting temperature and high solubility of RE ions [2-4]. The adding of metal oxides in phosphate glass network like Li_2O, Na_2O, K_2O, BaO and Al_2O_3 results in the formation of M-O(-P) bonds, which improves the mechanical strength, chemical durability and thermal stability of the phosphate glasses [1,5]. Trivalent erbium ions (Er^{3+}) doped glasses are interesting ion for obtaining laser emission, amplifier and up-converters in optical fibers for telecommunication due to their attribute emission at 1.54 μm that corresponds to $^4I_{13/2} \rightarrow {}^4I_{15/2}$ [6-8]. In this direction, many research works carried on Er^{3+} doped glass matrices such as germanate, oxyfluoride, tellurite and phosphate for optical amplifiers and includes some of the recent works on oxide glasses [6-9].

In this work, sodium aluminium phosphate glasses doped with Er^{3+} have been prepared. The physical, optical and luminescence properties were studied as a function of Er_2O_3 concentration. The luminescence and radiative properties of glass samples were investigated by Judd–Ofelt (JO) and McCumber's theory were subjected to find the long wavelength side of laser transition.

2. Experimental

Glass systems with composition of $15Na_2O$ - $20Al_2O_3$ - (65-x) P_2O_5 - xEr_2O_3 (x = 0.0, 0.05, 0.5, 1.0, 2.0 and 3.0 mol%) were prepared by melt quenching technique and title as NAPEr1, NAPEr2, NAPEr3, NAPEr4, NAPEr5 and NAPEr6, respectively. The batched mixture about 20 g is placed in a porcelain crucible and this homogenous mixture was heated in an electric furnace at 1200°C for 3 h. The melt was quenched by pouring it on to a preheated graphite mold and then annealed at 500°C for 3 h. Then the samples cooled down slowly to room temperature. At last, the prepared samples were cut and polished as shown in Figure 1.

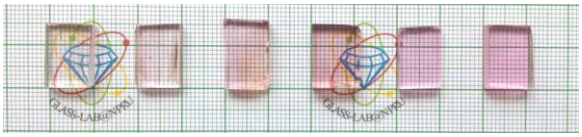

Figure 1. Photograph of the glass samples with different Er_2O_3 concentration.

DOI: 10.14456/jmmm.2019.19

The densities (ρ) of glass samples were measured by applying the Archimedes principle with four digits electric balance (AND, HR-200). The molar volume (V_m) was calculated by dividing the total molecular weight by its density of each sample. The value of refractive indices was recorded by an Abbe refractometer with a sodium-vapor lamp as a light source (598.3 nm) and having monobromonaphthalene as a contact liquid. The absorption spectra in the region of 200-1700 nm were recorded by UV-Vis-NIR spectrophotometer (shimadzu, UV-3600). The NIR luminescence emission spectra were recorded with phosphorescence/fluorescence spectro fluorometer (Quanta Master 300, Photon Technology International) using xenon lamp as a excitation source. The experimental oscillator strengths (f_{exp}) have been calculated by measuring the area under the absorption bands and using the following formula;

$$f_{\exp} = 4.32\times10^{-9}\int \varepsilon(v)\,dv \qquad (1)$$

where v is the wave number (cm^{-1}) of the transition from the ground state to the excited state and $\varepsilon(v)$ is the molar absorptivity of the transition. According to JO theory oscillator strength of an absorption band is given by

$$f_{cal} = \frac{8\pi^2 mcv}{3h(2J+1)}\frac{\left(n^2+2\right)^2}{9n}\sum_{\lambda=2,4,6}\Omega_\lambda\left|\left\langle \Psi J\left\|U^{(\lambda)}\right\|\Psi' J'\right\rangle\right|^2 \quad (2)$$

where $(n^2 + 2)^2/9n$ is a factor for the effective field at the well-localized center in a medium of isotropic refractive index, m is the mass of electron, c is the velocity of light in vacuum, h is the Planck's constant, n is the refractive index of glass, v is the frequency of the $\Psi J \rightarrow \Psi' J'$ transition, Ω_λ (λ = 2,4,6) are the JO intensity parameters and $\left\|U^{(\lambda)}\right\|^2$ are the doubly reduced matrix elements of the unit tensor operator of the rank λ = 2, 4 and 6 which are calculated from the intermediate coupling approximation for a transition $\Psi J \rightarrow \Psi' J'$. The three intensity parameters Ω_λ (λ = 2, 4 and 6) have been calculated by the least square fit method by applying JO theory to the experimental value of oscillator strength (f_{exp}) [2-5].

3. Results and discussion

3.1 Physical properties

The physical properties of the present glasses are shown in Table 1. The results show that the densities and refractive index of the glass samples tended to increase with increasing of Er_2O_3 concentration because of the changing of P_2O_5 (lower molecular weight 141.94 $g\cdot mol^{-1}$) by Er_2O_3 (higher molecular weight 382.52 $g\cdot mol^{-1}$) in glass composition. The increasing of refractive index due to the Er_2O_3 has higher density more than P_2O_5 and the increasing of the density also cause to the increasing of the refractive index, which can be explained by the dielectric theory [10]. The molar volume of glasses increases with increasing of Er_2O_3 contents up to 1.0 mol% thereafter decrease as can be seen in Table 1. The increasing of the molar volume due to the formation of non-bridging oxygen (NBO) when adding Er_2O_3 ions into glass network, which Er^{3+} acting as glass modifier of the glass network. While, the decrease of molar volume can be explained that the Er_2O_3 may diffuse to glass network and Er_2O_3 act as network former, leading to higher compactness and connectivity in glass structure.

3.2 Absorption spectra and oscillator strengths

The UV-Vis-NIR absorption spectra of different concentrations for Er^{3+} doped glass samples in the wavelength range of 200–1700 nm are displayed in Figure 2. The absorption peaks observed from the absorption spectra related to the transitions originated from $^4I_{15/2}$ ground state to the various excited states are presented in Table 2 [11]. The absorption peaks at 379, 522 and 1537 nm are the highest absorption peaks in UV, Vis and NIR region, respectively. Furthermore, the intensity of the absorption peak increase with increasing of Er^{3+} concentration.

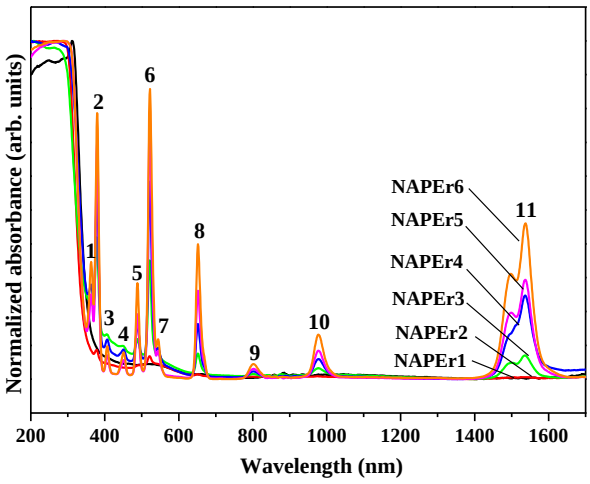

Figure 2. The absorption spectra of the glass samples with different Er_2O_3 concentration.

Table 1. Density, molar volume and refractive index of the glass samples.

Glass name	Density ($g\cdot cm^{-3}$)	Molar volume ($cm^3\cdot mol^{-1}$)	Refractive index
NAPEr1	2.617	46.597	1.5200
NAPEr2	2.598	46.996	1.5203
NAPEr3	2.620	47.002	1.5221
NAPEr4	2.643	47.049	1.5220
NAPEr5	2.701	46.938	1.5238
NAPEr6	2.752	46.937	1.5259

Table 2. The experimental (f_{exp}) and calculated (f_{cal}) oscillator strengths of NAPEr5 glass.

Peak number	Transitions $^4I_{15/2} \rightarrow$	Wavelength (nm)	Energy (cm^{-1})	f_{exp} ($\times 10^{-6}$)	f_{cal} ($\times 10^{-6}$)
1	$^4G_{9/2}$	363	27548	1.0825	0.0565
2	$^4G_{11/2}$	379	26385	1.5180	1.5027
3	$^4F_{3/2}$	406	24631	0.1212	0.0710
4	$^4F_{5/2}$	451	22173	0.1681	0.1534
5	$^4F_{7/2}$	488	20492	0.3675	0.5496
6	$^2H_{11/2}$	522	19157	2.1638	2.1888
7	$^4S_{3/2}$	544	18382	0.4610	0.2028
8	$^4F_{9/2}$	652	15337	0.4430	0.6134
9	$^4I_{9/2}$	802	12469	0.1031	0.5211
10	$^4I_{11/2}$	978	10225	0.2509	0.5366
11	$^4I_{13/2}$	1537	6506	1.6551	1.8122
δ_{rms} = 0.365					

3.3 NIR emission spectra, JO and radaitive parameter

Figure 3. shows the near infrared (NIR) luminescence spectra of NAPEr glasses in the wavelength range of 1400–1700 nm under 979 nm excitation wavelength. The NIR emission spectra have a strong peak at 1536 nm corresponding to the transition $^4I_{13/2} \rightarrow {}^4I_{15/2}$. The intensity of 1536 nm emission peak increases with increase in Er^{3+} ions concentration upto 2.0 mol% and after that decreases because of concentration quenching effect.

The observed absorption bands were utilized to calculate the experimental (f_{exp}) and calculated (f_{cal}) oscillator strengths of 2.0 mol% Er^{3+} ions doped with sodium aluminium phosphate glasses are listed in Table 2. A good agreement observed between f_{exp} and f_{cal} with overall δ_{rms} values of 0.365. Among all absorption bands, the $^4I_{15/2} \rightarrow {}^2H_{11/2}$ transition centered at 522 nm shows high intensity corresponding to high values of f_{exp} and f_{cal} of glasses, which is referred as the hypersensitive transition [12].

The JO parameters are very important for the study of local structure as well as bonding in the vicinity of RE ions. Generally, the Ω_2 intensity parameter is associated to the covalency of the RE–O bond as well as the asymmetry around the RE^{3+} ion site. The Ω_4 and Ω_6 intensity parameter are related to the viscosity, rigidity of the host matrix [13]. The JO parameters of NAPEr5 glass are found to be Ω_2 = 1.58 x 10^{-20} cm^2, Ω_4 = 0.14 x 10^{-20} cm^2 and Ω_6 = 0.48 x 10^{-20} cm^2 and follow the trend as $\Omega_2 > \Omega_6 > \Omega_4$ as shown in Table 3.

The radiative properties like spontaneous transition probability (A_R), stimulated emission-cross section (σ_e), branching ratio (β_R) and radiative lifetime (τ_R) were estimate using the formula reported in previous literature [14] and the calculated values are shown in Table 4. These parameters are important for spectroscopic characterization of Er^{3+} doped glasses for laser medium applications. The higher σ_e value corresponds to lower laser threshold and higher gain laser application. From Table 4, the higher value of σ_e point out specify that at 1536 nm transition can a good lasing transition and be useful for laser applications [15].

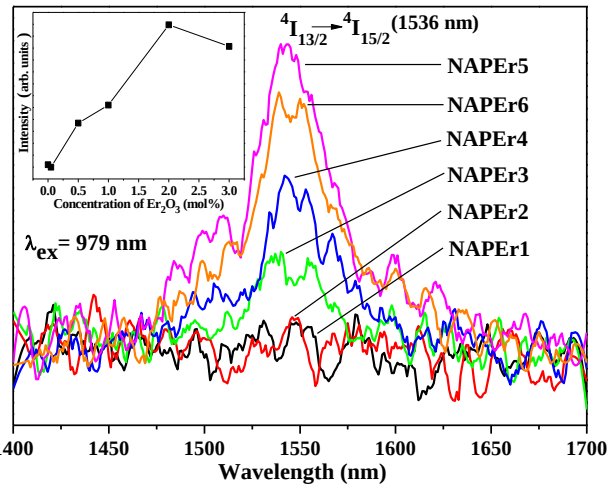

Figure 3. NIR photoluminescence spectra from $^4I_{13/2} \rightarrow {}^4I_{15/2}$ transition of NAPEr glasses.

Table 3. Judd–Ofelt parameters for different Er^{3+} doped glassy hosts.

Glass	Ω_2 ($\times 10^{-20}$ cm^2)	Ω_4 ($\times 10^{-20}$ cm^2)	Ω_6 ($\times 10^{-20}$ cm^2)	Trend
NAPEr5 [Present work]	1.58	0.14	0.48	$\Omega_2 > \Omega_6 > \Omega_4$
Telluro-fluoroborate [10]	1.77	0.28	0.70	$\Omega_2 > \Omega_6 > \Omega_4$
STB2.0E [14]	9.14	0.14	1.25	$\Omega_2 > \Omega_6 > \Omega_4$
2ErBiPbTB [15]	13.99	3.19	4.20	$\Omega_2 > \Omega_6 > \Omega_4$
E2YTBL [13]	7.23	1.46	1.57	$\Omega_2 > \Omega_6 > \Omega_4$
Zinc-Sodium-Tellurite [18]	1.08	0.35	0.41	$\Omega_2 > \Omega_6 > \Omega_4$

Table 4. Spontaneous transitionprobability (A_R, s^{-1}), stimulated emission-cross section ($\sigma_e \times 10^{-22}$, cm^2), branching ratio (β_R, %) and radiative lifetime (τ_R, ms) of NAPEr5 glass.

Glass system	λ (nm)	ΔE (cm^{-1})	A_R (s^{-1})	σ_e ($\times 10^{-22}$ cm^2)	β_R (%)	τ_R (ms)
NAPEr5 [Present work]	1537	6506	68.15	41.53	100	14.673
PKAZFEr20 [5]	1536	-	-	49.8	-	-
ZnAlBiBEr20 [15]	1530	-	-	9.38	-	-
2ErBiPbTB [16]	1532	-	-	84	-	-
$75TeO_2$–$20ZnO$–$3Na_2O$–$2Er_2O_3$ [19]	-	-	-	37.9	-	-

3.4 Visible luminescence spectra

From the NIR emission spectra show the concentration quenching effect at 2.0 mol% (NAPEr5) so NAPEr5 glass was chosen to study visible luminescence. Figure 4. shows the excitation spectra of NAPEr5 glass under the emission of 550 nm which consists of two excitation peaks that corresponding to the transitions from $^4I_{11/2} \rightarrow {}^4G_{11/2}$ (349nm) and $^4I_{11/2} \rightarrow {}^2G_{9/2}$ (403 nm). It is similar to reported literature [10]. Among the two excitation peaks it is observed that transition $^4I_{11/2} \rightarrow {}^2G_{9/2}$ (403 nm) is more intense and is used to record the emission spectra for the NAPEr5 glass under investigation. The emission spectra of glass sample show in Figure 5. It is observed from the figure that, two emissions at 525 and 548 nm corresponding to $^2H_{11/2} \rightarrow {}^4I_{15/2}$ and $^4S_{3/2} \rightarrow {}^4I_{15/2}$ transitions [10,16] respectively. From the emission spectra that, the $^4S_{3/2} \rightarrow {}^4I_{15/2}$ transition possess more intensity compared to the $^2H_{11/2} \rightarrow {}^4I_{15/2}$ transition due to the change in the coordination number of Er^{3+} ions in the glass sample [17].

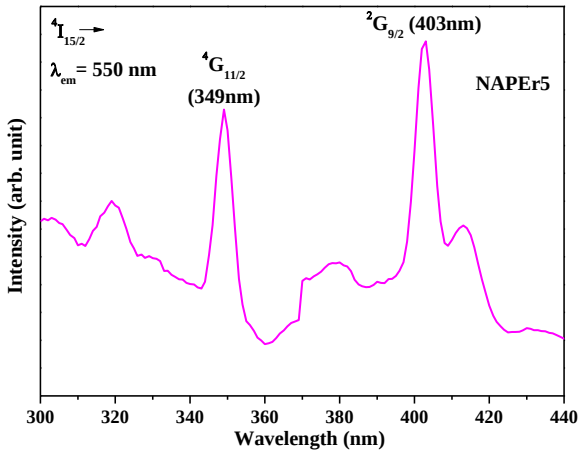

Figure 4. Excitation spectra of NAPEr5 glass under the emission of 550 nm.

3.5 Emission cross-section

The McCumber's theory explains the spectral overlap of absorption and emission cross-section using the absorption data near1536 nm. It can be expressed using the following by ref [2]. Mc Cumber theory is a powerful tool that permits one these two cross section to be calculated if the other is known from measurement. The relationship of absorption cross section to emission cross section for transition between two levels is given by the Mc Cumber relation

$$\sigma_{em}(\upsilon) = \sigma_{abs}(\upsilon)\exp\left(\frac{\varepsilon - h\nu}{K_B T}\right) \qquad (3)$$

where ε is the effective energy difference between the two manifolds, K_B is Boltzman's constant and T is the absolute temperature. Figure 6. Show the absorption and emission cross-sections ($^4I_{13/2} \rightarrow {}^4I_{15/2}$) transition in NAPEr5 glass. The values for peak absorption found to be 3.57×10^{-22} cm^2 and for emission cross-sections is 4.36×10^{-22} cm^2.

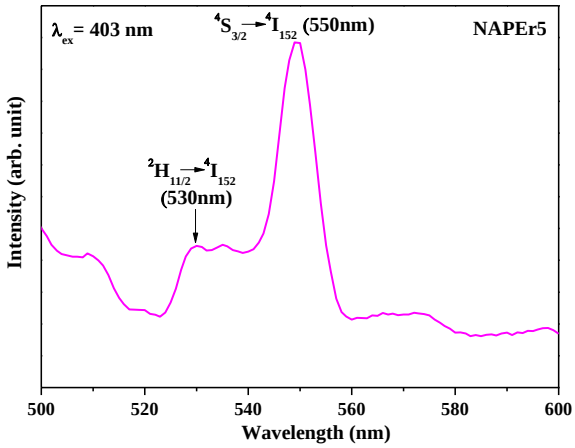

Figure 5. Visible emission spectra of NAPEr5 glass under the excitation of 403 nm.

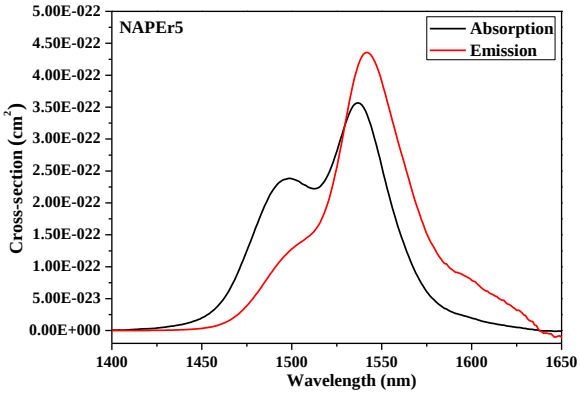

Figure 6. Absorption and emission cross-sections for $^4I_{13/2} \rightarrow {}^4I_{15/2}$ of Er^{3+} doped NAPEr5 glass calculated by the McCumber theory.

The σ_e calculated with JO theory (σ_e = 41.53 × 10^{-22} cm^2) is higher than that evaluated with McCumber theory (σ_e = 4.36 × 10^{-22} cm^2). The difference is due to the reabsorption caused by the spectral overlap of the emission and absorptions of Er^{3+} ions at 1536 nm.

4. Conclusions

The Er^{3+} doped sodium aluminuim phosphate glasses have been prepared with different concentration of Er_2O_3 for photonics material application. The density as well as refractive index tended to increase with increasing of Er_2O_3 concentration while, the molar volume decreased as Er_2O_3 concentration increased. The absorption spectra at 379, 522 and 1537 nm are highest absorption spectra in UV, Vis and NIR region, respectively. The spectroscopic properties of the prepared glasses were study with JO theory and the higher Ω_2 values of the prepared glasses show the higher asymmetry around the Er^{3+} ions. From the emission spectra that, the $^4S_{3/2}\rightarrow{}^4I_{15/2}$ transition possess more intensity compared to the $^2H_{11/2}\rightarrow{}^4I_{15/2}$ transition. The absorption and stimulated emission cross-sections were analyzed by using McCumber theory and the emission cross-section for the glass samples was found to be lower than PKAZFEr20 [5] and 2ErBiPbTB [17] but higher than ZnAlBiBEr20 [15] and $5TeO_2$–$20ZnO$–$3Na_2O$–$2Er_2O3$ [19]. The results disclose that the studied glasses might be potential candidates for photonic applications.

5. Acknowledgements

The author would like to thanks Center of Excellence in Glass Technology and Materials science (CEGM), Nakhon Pathom Rajabhat University (NPRU), Suan Sunandha Rajabhat University (SSRU) and National Research Council of Thailand (NRCT) for supporting this research.

References

[1] A. A. Reddy, S. S. Babu and G. V. Prakash, "Er^{3+} -doped phosphate glasses with improved gain characteristics for broadband optical amplifiers," *Optics Communications*, vol. 285, pp. 5364-5367, 2012.

[2] S. Hraiech, C. Bouzidi and M. Férid, "Luminescence properties of Er^{3+} -doped phosphate glasses," *Physica B*, vol. 522, pp. 15-21, 2017.

[3] M. Seshadria, K. Venkata Raoa, J. L. Raob, and Y. C. Ratnakaram, "Spectroscopic and laser properties of Sm^{3+} doped different phosphate glasses," *Journal of Alloys and Compounds*, vol. 476, pp. 263-270, 2009.

[4] M. Seshadri, M. Radha, D. Rajesh, L. C. Barbosa, C.M.B. Cordeiro, and Y. C. Ratnakaram, "Effect of ZnO on spectroscopic properties of Sm^{3+} doped zincphosphate glasses," *Physica B*, vol. 459, pp. 79-87, 2015.

[5] V. B. Sreedhar, N. Vijaya, D. Ramachari, and C. K. Jayasankar, "Luminescence studies on Er^{3+} -doped zincfluorophosphate glasses for 1.53 μm laser applications," *Journal of Molecular Structure*, vol. 1130, pp. 1001-1008, 2017.

[6] C. Basavapoornima, K. Linganna, C. R. Kesavulu, S. Ju, B. H. Kim, W. -T. Han, and C.K. Jayasankar, "Spectroscopic and pump power dependent upconversion studies of Er^{3+} -doped lead phosphate glasses for photonic applications," *Journal of Alloys and Compounds*, vol. 699, pp. 959-968, 2017.

[7] K. Maheshvaran, S. Arunkumar, K. Venkata Krishnaiah, and K. Marimuthu, "Investigations on luminescence behavior of Er^{3+}/Yb^{3+} co-doped boro-tellurite glasses, "*Journal of Molecular Structure*, vol. 1079, pp. 130-138, 2015.aa

[8] D. Yin, S. Peng, Y. Qia, S. Zheng, Y. Zhou, and X. Wang, "Enhancement of the 1.53 μm fluorescence and energy transfer in Er^{3+}/Yb^{3+}/Ce^{3+} tri-doped WO_3 modified tellurite-based glass," *Journal of Alloys and Compounds*, vol. 581, pp. 534-541, 2013.

[9] F. Ahmadi, R. Hussin, and S. K. Ghoshal, "Spectral characteristics of Er^{3+} doped magnesium zinc sulfophosphate glasses," *Journal of Alloys and Compounds*, vol. 711, pp. 94-102, 2017.

[10] N. Luewarasirikul, N. Chanthima, Y. Tariwong, and J. Kaewkhao, "Erbium-doped calcium barium phosphate glasses for 1.54 μm broadband optical amplifier" *Materials Today: Proceedings*, vol. 5, pp. 14009-14016, 2018.

[11] W. T. Carnall, P. R. Fields and K. Rajnak, "Electronic Energy Levels in the Trivalent Lanthanide Aquo Ions. I. Pr^{3+}, Nd^{3+}, Pm^{3+}, Sm^{3+}, Dy^{3+}, Ho^{3+}, Er^{3+}, and Tm^{3+}," *The Journal of Chemical Physics*, vol. 49, pp. 4424-4442, 1968.

[12] J. J. Leal, R. Narro-García, H. Desirena, J. D. Marconi, E. Rodríguez, K. Linganna, and E. DelaRosa, "Spectroscopic properties of tellurite glasses co-doped with Er^{3+} and Yb^{3+}," *Journal of Luminescence*, vol. 162, pp. 72-80, 2015.

[13] C. R. Kesavulu, H. J. Kim, S. W. Lee, J. Kaewkhao, N. Wantana, S. Kothan and S. Kaewjaeng, "Influence of Er^{3+} ion concentration on optical and photoluminescence properties of Er^{3+} -doped gadolinium-calcium silica borate glasses," *Journal of Alloys and Compounds*, vol. 683, pp. 590-598, 2016.

[14] K. Annapoorani, N. SuriyaMurthy, T. R. Ravindran, and K. Marimuthu, "Influence of Er^{3+} ion concentration on spectroscopic properties and luminescence behavior in Er^{3+}

doped Strontium telluroborate glasses," *Journal of Luminescence*, vol. 171, pp. 19-26, 2016.

[15] K. Swapna, S. K. Mahamuda, M. Venkateswarlu, A. SrinivasaRao, M. Jayasimhadri, S. Shakya, and G. VijayaPrakash, "Visible, Up-conversionand NIR (1.5 μm) luminescence studies of Er^{3+} doped Zinc Alumino Bismuth Borate glasses," *Journal of Luminescence*, vol. 163, pp. 55-63, 2015.

[16] S. K. Nayab Rasool, B. C. Jamalaiah, K. Suresh, L. Rama Moorthy, and C. K. Jayasankar, "Spectroscopic properties of Er^{3+}-doped phosphate based glasses for broadband 1.54 μm emission," *Journal of Molecular Structure*, vol. 1130, pp. 837-843, 2017.

[17] S. Arunkumar and K. Marimuthu, "Spectroscopic properties of Er^{3+} doped bismuth leadtelluroborate glasses for 1.53 μm optical amplifiers," *Journal of Alloys and Compound*, vol. 627, pp. 54-68, 2015.

[18] S. Y. Moustafa, M. R. Sahar, and S. K. Ghoshal, "Spectroscopic attributes of Er^{3+} ions in antimony phosphate glass incorporated with Ag nanoparticles: Judd-Ofelt analysis," *Journal of Alloys and Compounds*, vol. 712, pp. 781-794, 2017.

[19] A. A. Assadi, K. Damak, R. Lachheb, A. Herrmann, E. Yousef, C. Rüssel, and R. Maâlej, "Spectroscopic and luminescence characteristics of erbium doped TNZL glass for lasing materials," *Journal of Alloys and Compounds*, vol. 620, pp. 129-136, 2015.